CHEMISTRY
A EUROPEAN JOURNAL

DOI: 10.1002/chem.200800182

Preparation of Highly Active and Dispersed Platinum Nanoparticles on Mesoporous Al-MCM-48 and Their Activity in the Hydroisomerisation of *n*-Octane

Juan M. Campelo,[a] Adam F. Lee,[b] Rafael Luque,*[a, c] Diego Luna,[a] Jose M. Marinas,[a] and Antonio A. Romero[a]

Abstract: Platinum nanoparticles supported on Al-MCM-48 materials have been prepared. The resultant catalysts have been characterized by means of XRD, N_2 physisorption experiments, scanning electron microscopy (SEM), transmission electron microscopy (TEM), temperature-programmed reduction (TPR), and diffuse reflectance infrared Fourier-transform spectroscopy (DRIFTS). The activity of these nanoparticles has been tested in relation to the hydroisomerisation of *n*-octane. The catalytic activities were typically 50%, with selectivities in the isomerisation process in excess of 70%, favouring the formation of the 3-methylheptane isomer with respect to the 2- and 4-methylheptanes.

Keywords: alkanes · heterogeneous catalysis · isomerisation · nanoparticles · platinum

Introduction

Environmental regulations have restricted the content of aromatic and alkenic hydrocarbons in gasolines, which have a detrimental effect on their production as well as on their octane numbers. Light isoalkanes are required for the production of more environmentally friendly and high-octane-number gasolines. *n*-Alkanes are isomerised to increase the octane number in the naphtha (transformation of linear-chain paraffins to branched isomers with high octane numbers) as well as to induce significant improvements in several physical properties of the gasoline, including the pour point and viscosity.[1]

Much effort has been devoted to the isomerisation of longer C_7 chain alkanes in the last few years, and it has become an interesting research avenue for both academic researchers and industrial partners.[2–5] Akhmedov et al. have recently reviewed the salient advances with regard to the selective isomerisation of longer C_7 chain alkanes.[2] The conversion of longer C_7 chain alkanes is not trivial as there are two different and competing pathways, namely isomerisation and cracking. The conventional reaction mechanism is monomolecular. Alkanes are dehydrogenated on the metallic phase, and the alkenes generated are protonated on the acidic sites of the catalyst to form alkylcarbenium ions. The reaction (either isomerisation or cracking of the alkane) then takes place on the acidic sites, and the alkene generated in the process is hydrogenated at the nearby metallic sites, affording the isomerised-fragmented *n*-alkane (Scheme 1). Thus, it is rather challenging to obtain high selectivities in favour of branched isomers without an appreciable selectivity in favour of cracking. The β-scission of long-chain paraffins has been reported to be the main reason for this phenomenon.[6] Consequently, the preparation of materials with improved activities and selectivities favouring the isomerisation of long-chain paraffins is highly desirable. Hydroisomerisation reactions are generally performed over bifunctional catalysts having a noble metal function, which is usually involved in hydrogenation–dehydrogenation processes, and acidic sites, which are involved in C–C skeleton rearrangements. The major parameters influencing the reaction selectivity are the pore structure[7–9] and the acidity.[10–12] The key to the successful preparation of active and selective cat-

[a] Prof. J. M. Campelo, Dr. R. Luque, Prof. D. Luna, Prof. J. M. Marinas, Dr. A. A. Romero
Departamento de Química Orgánica, Facultad de Ciencias
Universidad de Córdoba, Campus Universitario de Rabanales
Edificio Marie Curie, 14014 Córdoba (Spain)
E-mail: rla3@york.ac.uk

[b] Dr. A. F. Lee
Department of Chemistry, The University of York
Heslington, YO10 5DD, York (UK)

[c] Dr. R. Luque
Current address: Green Chemistry Centre of Excellence
The University of York
Heslington, YO10 5DD, York (UK)
Fax: (+44) 190-443-2705

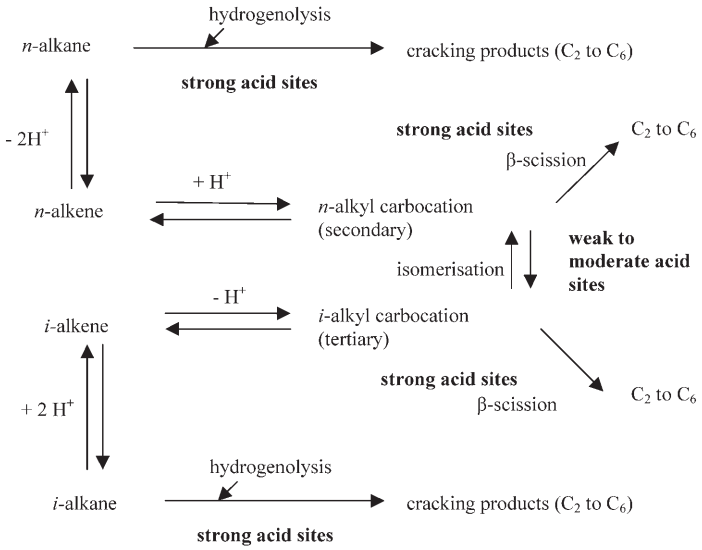

Scheme 1. *n*-Alkane hydroisomerisation reaction mechanism.

alysts lies in the selection of a mild acidity (to minimise the production of cracking products) together with a highly active metallic function (e.g. Pt, Pd, Ni), which improves the selectivity in favour of isomerisation. Among the noble metals, Pt has been shown to considerably increase the selectivity in favour of isomerisation, and is therefore the most suitable metal for the hydroconversion of *n*-alkanes.[2]

Various catalysts have been reported to be active in the hydroisomerisation of C_7 and longer C_7 chain *n*-alkanes, including materials based on MoO_3,[13] Pt-WO_3-ZrO_2,[4,14–17] Al-MCM-41,[18,19] zeolite-supported Pt,[20–23] and Pt–silicoaluminophosphates (SAPO) materials[8,9,24] as alternatives to the traditional Pt and Re/Al_2O_3 catalysts. In particular, compared to microporous zeolites, Al-MCM-41 materials have a moderate acidity, and the incorporation of metallic sites into these materials (e.g. Zr, Pt) produces solid catalysts that have proved to be highly active and selective in the isomerisation of C_6 and C_7 alkanes.[18,19] The optimum loading of metal (Pt or Zr) in these materials was found to be close to 0.3 wt%, whereas Campelo et al. reported that a 0.5 wt% Pt content gave catalysts with optimum activity and selectivity in favour of isomerisation.[9] We have also recently reported the preparation of catalytically active Al-MCM-48 solid acids for use in various reactions.[25] These materials showed great potential for use as catalysts and supports in a wide range of applications.

Herein, we report the synthesis of platinum nanoparticles supported on Al-MCM-48 and their catalytic performance in the hydroisomerisation of *n*-octane.

Experimental Section

The preparation of the Al-MCM-48 has been reported previously.[25] The synthesis of the supported Pt materials involved some different steps. Firstly, the appropriate amount of tetraamine platinum(II) nitrate for the chosen Pt loading in samples (typically 0.5 wt%) was dissolved in ethanol and subsequently mixed with the Al-MCM-48, stirring the mixture in a rotary evaporator at 40°C for a few hours. Ethanol acts as the reducing agent in the deposition of the Pt nanoparticles.[26] The materials were then calcined in air (60 mL min^{-1}) at 400°C for 2 h and then reduced in hydrogen (100 mL min^{-1}) at 400°C for 3 h. The Pt/Al-MCM-48 catalysts are denoted as 0.5%Pt-XAl, where 0.5 wt% is the approximate Pt loading and X (40 to 15) is the theoretical Si/Al ratio (in the synthesis gel) of the Al-MCM-48 support. Materials with different Pt loadings (ranging from 0.5 to 5% Pt) were also prepared for comparative purposes. A 0.5 wt% Pt loading was chosen as we have previously reported this to be ideal for obtaining catalysts with optimum activity and selectivity in favour of the isomerisation process.[9]

Characterization of the materials: Powder X-ray diffraction patterns (XRD) were recorded on a Bruker AXS diffractometer employing $Cu_{K\alpha}$ radiation ($\lambda = 1.5418$ Å), over a 2θ range from 2 to 10°, with a step size of 0.02° and counting time per step of 1 s. Extended scans were performed over a 2θ range of 5 to 85°, with a step size of 0.01° and a counting time per step of 4 s.

Nitrogen physisorption was measured with a Micromeritics ASAP 2000 instrument at −196°C. Samples were degassed for 2 h at 100°C under vacuum ($p < 10^{-2}$ Pa) and subsequently analysed. The linear part of the BET equation (relative pressure between 0.05 and 0.22) was used for the determination of the specific surface area. The pore size distribution (PSD) was calculated from the adsorption branch of the N_2 physisorption isotherms employing the Barret–Joyner–Halenda (BJH) formula. The cumulative mesopore volume, V_{BJH}, was obtained from the PSD curve.

Scanning electron micrographs (SEM) and elemental compositions of the calcined samples were obtained using a JEOL JSM-6300 scanning microscope with energy-dispersive X-ray analysis (EDX) at 20 kV. Samples were coated with Au/Pd on a high-resolution SC7640 sputterer at a sputtering rate of 1500 V per minute, up to a thickness of 7 nm.

Transmission electron microscopy (TEM) micrographs were recorded on an FEI Tecnai G^2 fitted with a CCD camera for ease and speed of use. The resolution was around 0.4 nm. Samples were suspended in ethanol and immediately deposited on a copper grid prior to analysis.

Diffuse reflectance Fourier-transform infrared spectra (DRIFTS) were recorded on a Bomem MB series instrument equipped with an environmental chamber (Spectra Tech, P/N 0030–100) placed in the diffuse reflectance attachment (Spectra Tech, Collector). The environmental chamber allows precise control of the temperature, pressure, and the environment of the sample, as well as ensuring reproducibility of the experiments. The resolution was 8 cm^{-1}, and 256 scans were averaged to obtain spectra in the 4000–400 cm^{-1} range. Samples were dried at 150°C for 24 h, mixed with KBr to 15 wt%, placed in the environmental chamber under a 20 mL min^{-1} flow of air, heated to 300°C, and held at this temperature for 1 h prior to measuring the spectra.

Surface acidity was measured in dynamic mode by means of a pulse chromatographic technique involving gas-phase (300°C) adsorption of pyridine (PY; sum of Brønsted and Lewis acid sites) and 2,6-dimethylpyridine (DMPY; Brønsted sites) as probe molecules, using a method previously described elsewhere.[25]

The experimental procedure used for temperature-programmed desorption of pyridine (PY-TPD) has also been reported previously.[25] The apparatus used for pyridine adsorption/desorption was basically a modified gas chromatograph. The catalyst (ca. 50 mg) was packed into a stainless steel tube of length 100 mm and diameter 4 mm, and retained therein between quartz wool plugs. Pure N_2 at a flow rate of 50 mL min^{-1} was used as the carrier gas. Prior to the adsorption experiments, the catalyst was pretreated in situ by passing pure N_2 through it at a flow rate of 50 mL min^{-1} and heating from 50 to 450°C at 10°C min^{-1} (the temperature was maintained at 450°C for 10 min). The temperature was then lowered to 100°C and the adsorption experiment was carried out. Py-TPD experiments were performed in the 50–700°C range after saturation of the sample followed by purging in N_2 at 100°C for 1 h.

Specific platinum surface areas and associated metal dispersions were measured by H_2 chemisorption using a Micromeritics 2700 PulseChemi-

sorb surface area analyser. Samples were pre-reduced at 400 °C for 1 h and then cooled under an Ar stream prior to measurement by the pulse chemisorption method. Temperature-programmed reduction (TPR) was conducted on a Stanton-Redcroft STA 750 thermal analyser under a 10 vol% H_2/He stream at a total flow rate of 20 mL min^{-1} and with a ramp rate of 12 °C min^{-1} between room temperature and 800 °C.

Catalytic reactions (typically with 0.1 g of catalyst) were carried out in a continuous-flow system with PC control at 375 °C, employing hydrogen as carrier (25 mL min^{-1}) at 5 bar. The *n*-octane (50 μL min^{-1}, 0.31 mmol min^{-1}) was fed into the system by means of a peristaltic pump. Reaction products were identified and characterised by GC and GC-MS.

Results and Discussion

In general, the X-ray diffraction patterns of the Al-MCM-48 materials with supported platinum exhibited the characteristic lines of MCM-48 materials (Figure 1).[25,27] The diffraction lines at high 2θ angles (Figure 1, inset) can be assigned to the typical *fcc* platinum metal by comparison with the JCPDS card (No. 04-0802). The intensity of the Pt lines is relatively low due to the extremely high dispersion and low metal loading. Table 1 summarises the textural properties of the Pt/Al-MCM-48 materials.

Pt/Al-MCM-48 materials display similar textural properties to those of the parent materials,[25] including high surface areas and pore volumes, as well as pore diameters of the order of 2 nm. Typical type IV isotherm profiles, characteristic of mesoporous materials, were also obtained for all of these materials. Elemental analyses of the mesoporous supported materials showed that their Si/Al ratios remained almost unaltered compared with those of the parent materials.[25] Therefore, the platinum, which was present in very low quantities (less than 1%), is believed to be incorporated into the Al-MCM-48 materials. The interaction of the Pt with the silicon or aluminum on the surface remains unclear, although the presence of the Pt at such low loadings seemed to increase the acidity of the materials (refer to Table 3 and the PY-DRIFTS data).

TG-DTA and DRIFTS analyses of the materials bearing supported Pt showed similar profiles to those of the parent Al-MCM-48 materials.[25] SEM micrographs of Pt/Al-MCM-48 (Figure 2) were similar to those of the Al-MCM-48 materials, showing particles of spherical morphology that were very homogeneously distributed in terms of particle size and texture.

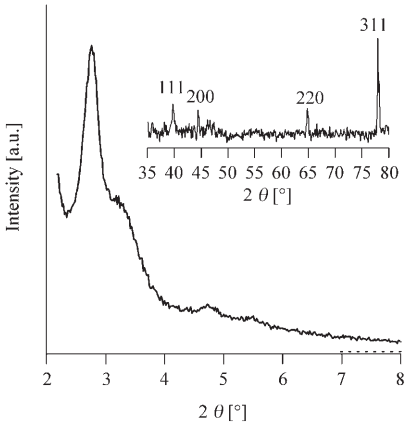

Figure 1. XRD patterns of 0.5% Pt-40Al material. The diffractogram in the inset features the various diffraction lines of metallic platinum.

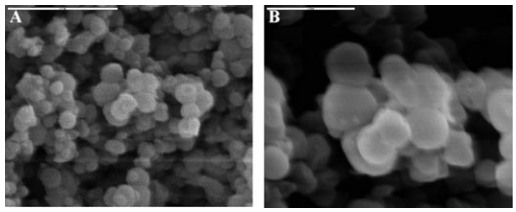

Figure 2. SEM micrographs of 0.5% Pt-30Al at different magnifications; a) ×20000 and b) ×30000.

Temperature-programmed reduction confirmed that only reduced Pt was present in all of the samples, irrespective of the metal loading or MCM composition. Decomposition of the amine ligands of the tetraamine platinum(II) nitrate employed as precursor upon calcination may provide a reductive environment conducive to the reduction of the metal nanoparticles and the formation of protons.[28] Specific metal surface areas allowed the Pt dispersions to be calculated (Table 2), and these exhibited only a weak dependence on the Al content. The Pt nanoparticles were found to be well dispersed at low metal loadings. Increased Pt loadings led to materials with a relatively low metal dispersion (Table 2, entries 6 and 7).

TEM micrographs of the Pt nanoparticles are shown in Figure 3. The mesoporous materials exhibited a highly dispersed particle distribution with a relatively narrow particle diameter range (Figure 3), in good agreement with the dispersion values obtained (Table 2). It should be noted that H_2 chemisorption measurements necessitate a pre-reduction step at 400 °C to remove any passivating surface oxide; this could potentially initiate Pt sintering over weakly interacting supports, leading to an underestimation of the true dispersion. However, the good agreement between particle size estimates for the high

Table 1. Textural properties including d_{211} spacing, unit cell parameter (a_o), surface area (S_{BET}), pore diameter (D_{BJH}), pore volume (V_{BJH}), and wall thickness (ε) of Pt/Al-MCM-48 materials.

Catalyst	d_{211} [nm]	a_o[a] [nm]	S_{BET} [m^{2}g^{-1}]	D_{BJH} [nm]	V_{BJH} [mL g^{-1}]	ε [nm]	Pt loading[b] [%]	Actual Si/Al ratio[b]
0.5% Pt-40Al	3.3	8.0	1261	1.9	0.53	1.5	0.43	51
0.5% Pt-30Al	3.4	8.2	1408	1.9	0.43	1.6	0.50	41
0.5% Pt-20Al	3.4	8.2	1009	2.1	0.75	1.6	0.56	26
0.5% Pt-15Al	3.5	8.6	1100	2.1	0.72	1.9	0.53	22

[a] Cubic unit cell parameter estimated as $a_o = d_{211}\sqrt{6}$. [b] The atom% of Pt and Si/Al ratio were determined by elemental analysis (EDX).

Table 2. Pt dispersion (obtained from H_2 chemisorption) and average nanoparticle sizes obtained from XRD (Scherrer equation; $d = 0.9\lambda / B\cos\theta$) and TEM (averaging 50 particles from the TEM micrographs) of various mesoporous Al-MCM-48-supported platinum materials.

Entry	Catalyst	Dispersion [%]	Average particle size (estimated from XRD) d [nm]	Average particle size (estimated from TEM) [nm]
1	0.5 % Pt-40Al	92	4.0	4.4
2	0.5 % Pt-30Al	81	4.3	4.8
3	0.5 % Pt-20Al	89	3.9	4.2
4	0.5 % Pt-15Al	70	4.7	4.4
5	1 % Pt-40Al	77	4.8	4.6
6	3 % Pt-40Al	40	5.1	5.2
7	5 % Pt-40Al	25	5.9	5.9

loading samples from the dispersion values in Table 2 (using the methodology of ref. [29] and assuming an equal ratio of (111):(110):(100) facets) and the associated TEM analysis suggests that the reported dispersions are accurate.[29] The extremely high dispersion of the lowest loading (0.5 % Pt) sample indicates a significant number of sub-nanometre clusters, which fall below the sensitivity of both powder XRD and the TEM system. The nanoparticle morphology was found to be spherical, with an average particle diameter of around 4.4 nm, as calculated from the TEM micrographs. These results are in good agreement with the particle sizes estimated from the XRD patterns using the Scherrer equation (Table 2). An increase in Pt loading from 0.5 to 5 wt % increased the average nanoparticle size (Table 2) and some big metal clusters (ca. 10–15 nm) could be observed in the materials with increased Pt loading (Figure 3B and C).

The catalysts exhibited surface acidities similar to those of the parent materials,[25] although slightly more acidic compared to Al-MCM-48 (Table 3). The incorporation of Pt seemed to increase the acidity of the materials. Of note was the unexpectedly high acidity of the Pt material with an Si/Al ratio of 40 (0.5 % Pt-40Al), which also exhibited the highest dispersion (92 %, Table 2). Such an increase in acidity compared to the parent Al-MCM-48 is, however, difficult to rationalise. A synergistic effect between the Pt and acidic sites in the materials might be present (even at low Pt loadings), which might be related to the decomposition of the Pt amine precursor complex and its interaction with the surface through the formation of the metal nanoparticles and protons.[28] On the other hand, the adsorbed aromatic bases, including PY and DMPY, might also interact with the Pt species through the formation of a complex, thereby increasing the quantity of base adsorbed on the surface of the materials. The metal–support interaction has also been reported to influence the acidity of supported Pt materials.[28,30] Interestingly, the platinised materials exhibited similar total (PY data) and Brønsted (DMPY data) acidities (Table 3), regardless of the Si/Al ratio, with the exception of the 0.5 % Pt-20Al sample. Pt-SAPO materials display a much higher density of acid sites compared to the Pt/Al-MCM-48 catalysts.

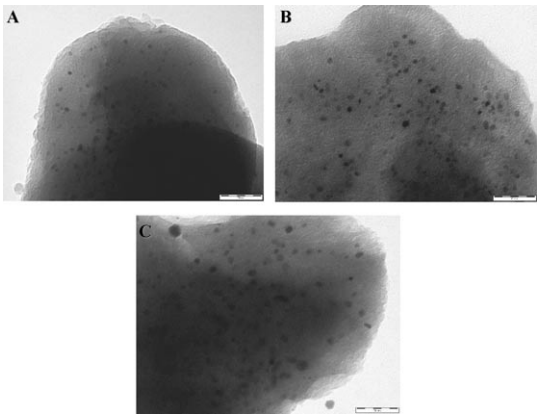

Figure 3. TEM micrographs (×300 000, 50 nm scale bar) of Pt/Al-MCM-48 materials. A) 1 % Pt-40Al; B) 3 % Pt-40Al; C) 5 % Pt-40Al.

Table 3. Surface acidity, measured by PY and DMPY titration (μmol probe molecule per g of catalyst and μmol probe molecule per m^2 at 300 °C) and Brønsted-Lewis ratio (measured by PY-DRIFTS) of Pt/Al-MCM-48 materials, compared to the values reported for Pt-SAPO materials.

Catalyst	PY [μmol g^{-1}]	PY [μmol m^{-2}]	DMPY [μmol g^{-1}]	DMPY [μmol m^{-2}]	B/L ratio (150 °C, DRIFTS)
40Al	133	0.09	74	0.05	0.9
0.5 % Pt-40Al	399	0.32	119	0.09	1.3
30Al	213	0.16	146	0.11	1.1
0.5 % Pt-30Al	360	0.26	127	0.09	1.4
20Al	241	0.17	99	0.07	1.2
0.5 % Pt-20Al	210	0.21	74	0.07	1.4
15Al	244	0.18	81	0.06	1.3
0.5 % Pt-15Al	397	0.36	126	0.11	1.3
0.5 % Pt-SAPO5	149	0.82	89	0.49	–
0.5 % Pt-SAPO11	68	0.66	16	0.16	–

Typical traces from PY-TPD experiments are shown in Figure 4. The PY desorption trace was deconvoluted using a Gaussian function with temperature as a variable. Experimental data, the individual components obtained by deconvolution, and the theoretical spectrum obtained by summing the individual peaks (standard deviations < 6 %) for Pt/Al-MCM-48 materials are compared to those of Al-MCM-48 in Figure 4 (scaled-up for comparative purposes). Peaks present at low temperature (around 210 and 290 °C) can be assigned to weakly to moderately acidic sites, having a major contribution to the acidity of the materials.[25] Peaks at higher temperatures (ca. 460 and 660 °C, respectively) can be attributed to more strongly acidic sites (Brønsted and Lewis) on the materials. In general, peaks were found to be slightly shifted to higher temperatures in the supported Pt materials compared to Al-MCM-48, and only a small decrease in peak intensity and contribution (area %) was found for Pt/Al-MCM-48 materials compared to Al-MCM-48 (Figure 4).[25]

PY-DRIFTS measurements were also performed to complete the surface acidity studies of the materials. The results

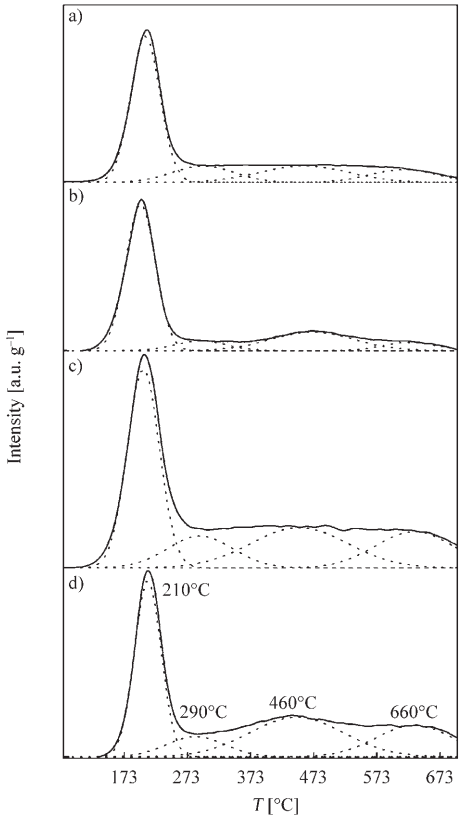

Figure 4. TPD profiles of mesoporous MCM-48 materials: a) 40Al, b) 0.5 % Pt-40Al, c) 20Al, and d) 0.5 % Pt-20Al.

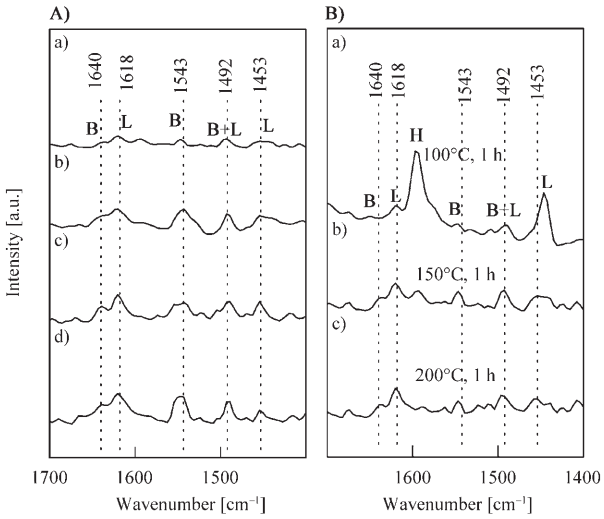

Figure 5. DRIFTS of adsorbed pyridine (1700–1400 cm^{-1}) at 150 °C. A) Al-MCM-48 and 0.5 % Pt/Al-MCM-48 materials; a) 40Al, b) 0.5 % Pt-40Al, c) 15Al, and d) 0.5 % Pt-15Al; B) 0.5 % Pt-40Al at different Py desorption temperatures; a) 100 °C, b) 150 °C, and c) 200 °C.

are presented in Figure 5 and Table 3. The mesoporous supported catalysts exhibited several peaks due to pyridine bound at Lewis sites (1618 and 1453 cm^{-1}), peaks due to pyridine bound at Brønsted acid sites (1640 and 1543 cm^{-1}), and a band at 1492 cm^{-1} attributable to pyridine interacting with both Lewis and Brønsted acid sites.[31] The desorption of PY at increasing temperatures results in the removal of both Brønsted-bound and Lewis-bound PY. The Pt materials exhibited analogous spectra to that of Al-MCM-48, featuring bands with similar intensities, except in the case of the 0.5 % Pt-40Al sample, for which a large increase in the intensity of the DRIFTS bands was found, in good agreement with the PY titration data. The Brønsted-Lewis ratio in the platinised materials was found to be very similar between samples, regardless of the aluminum content (Table 3).

The activity of the nanoparticles was then investigated in relation to the hydroisomerisation of *n*-octane. The hydroisomerisation of *n*-alkanes is a very complex catalytic process, which involves several parallel, competing, and consecutive reactions, including hydrogenations, isomerisations, and cracking reactions. Therefore, a great multitude of diverse products is generated (Scheme 1). The kinetics of these processes may be subjected to various approximations. The rate of reaction of the reactant is the key approximation to take into account, as reported previously.[32] In an ideal bifunctional catalyst, the metal phase only (de)hydrogenates, while the rate-determining step is the rearrangement and/or scission of the intermediates at the acidic sites.

Very low octane conversion was found at temperatures below 300 °C. Therefore, 350 °C was chosen as the optimum temperature for studying the activity of the Pt nanoparticles. The typical *n*-octane conversion values for the Pt/Al-MCM-48 systems were 50 %, comparable to those of Pt-SAPO materials with similar Pt content (Table 4)[9] and higher than that of the Al-MCM-48 parent material, in good agreement with the acidity data (Table 3). The parent Al-MCM-48 exhibited activities between 20 and 30 %, and almost complete selectivity in favour of the cracking products (mainly C_2 to C_5). These materials proved to be very efficient in the cracking of isopropylbenzene.[25]

Selectivities in the isomerisation process were higher than 70 %, favoring the formation of the 3-methylheptane isomer over the 2- and 4-methylheptanes (Tables 4 and 5). Interestingly, 2-methylheptane is preferentially obtained with Pt-SAPO catalysts. The aluminum content did not have a marked effect on either the conversions or the selectivities, in good agreement with the titration data (Table 3), which showed the Lewis and Brønsted acidities to be very similar in the supported Pt materials regardless of the Si/Al ratio. Only a slight decrease in conversion was found for the 0.5 % Pt-20Al catalyst as compared to the others (Table 4). The 0.5 % Pt-40Al catalyst was unexpectedly active in the hydroisomerisation reaction on the basis of its high Si/Al ratio. Nevertheless, the high activity of this material can be correlated to its high acidity (Table 3, Figure 5). A higher selectivity in favour of the C_7-isomers was also found at longer reaction times; this increased selectivity was achieved at the expense of the selectivity in favour of cracking. This outcome is most likely to stem from the decrease in the conversion. The most plausible explanation is that the more strongly acidic sites present in the support (mainly Brønsted), re-

Table 4. Total conversions (X_T, mol%) and selectivities in favour of cracking (S_{CK}, mol%) and isomerisation to methylheptanes (S_{MH}, mol%), including 2-, 3-, and 4-methylheptanes, of different materials in the hydroisomerisation of *n*-octane.[a]

Catalyst	4 h reaction			12 h reaction			20 h reaction		
	X_T	S_{CK}	S_{MH}	X_T	S_{CK}	S_{MH}	X_T	S_{CK}	S_{MH}
0.5%Pt-40Al	50	18	75	48	17	77	48	18	79
0.5%Pt-30Al	52	28	69	49	27	70	48	19	73
0.5%Pt-20Al	44	17	75	36	14	80	35	14	81
0.5%Pt-15Al	54	26	70	52	21	72	51	15	80
15Al	28	>95	–	25	>95	–	24	>95	–
0.5%Pt-SAPO5	50	79	21	45	76	24	41	65	35
0.5%Pt-SAPO11	28	33	59	25	29	64	21	26	74

[a] $T=375\,^{\circ}C$, $p=5$ bar, 0.1 g catalyst, $WHSV=12.7\ h^{-1}$; the fact that the selectivities do not total 100 is due to toluene (ethylbenzene was also obtained in small quantities).

sponsible for the formation of cracking products, are steadily deactivated with time due to the strong adsorption of carbonaceous species and/or the generated products (e.g., arenes and cyclohexane) on the catalyst surface.[33,34] Moderately and weakly acidic sites, responsible for the isomerisation phenomenon, are less prone to such deactivation, so an increase in the formation of C_7-isomers is observed with a concomitant decrease in the formation of cracking products.

Propane, butane, pentane, and hexane were obtained as cracking products (mainly C_2 to C_4; Table 5). The relatively low acidity of Al-MCM-48 materials accounts for the fact that the formation of such products, which usually takes place at the strongly acidic centres of the support, is not prominent under milder reaction conditions. Increasing concentrations of cracking products start to appear at higher temperatures, in good agreement with the classical consecutive hydroisomerisation mechanism.[35] No multibranched products were detected. Of note was the 1:2:1 relative ratio of the 2-, 3-, and 4-methylheptanes (Tables 5 and 6). The quantity of 3-methylheptane in the reaction product mixture thus corresponds to the sum of the quantities of the 2- and 4-isomers produced. This ratio was found to be constant and consistent for all of the Pt/Al-MCM-48 materials, regardless of the aluminum content or the reaction time.

The most important step in the hydroconversion of *n*-alkanes is the rearrangement of the intermediate alkyl carbocations (Scheme 1). The skeletal isomerisation of such carbenium ions was originally proposed to involve propanated cyclopropane (PCP) intermediates,[36,37] and this is generally accepted for alkanes larger than *n*-butane. According to the PCP mechanism, 3-methylheptane will be formed in preference to the 2-methyl isomer, in good agreement with the reported experimental results.[38,39] We can therefore conclude that the skeletal isomerisation of the intermediate *n*-alkyl carbocations is likely to proceed according to the PCP mechanism as this would account for the 1:2:1 relative ratio of the 2-, 3-, and 4-methylheptanes.

We then proceeded to investigate the effects of various parameters, including the hydrogen pressure, temperature, and Pt loading, on the performance of Pt/Al-MCM-48 in the hydroisomerisation of *n*-octane.

The hydrogen pressure in the continuous-flow reactor was found to be a critical parameter in determining the activity and selectivity of the Pt nanoparticles. The activities of Pt/Al-MCM-48 were investigated at four different hydrogen partial pressures within the reactor (1, 3, 5, and 7 bar, respectively, at 375 °C; 20 h reaction). The results are summarized in Table 6.

In general, an increase in the H_2 pressure in the systems increased the total conversion of starting material (the conversion was doubled on going from 1 to 5 bar), regardless of the aluminum content. Contrary to the observed trends, Chaudhari et al. reported a decrease in activity with increasing hydrogen partial pressures, as a result of rapid hydrogenation of the intermediate alkenes and carbocations, thereby preventing further reactions.[19] Nevertheless, we believe that an increase in the partial pressure of hydrogen activates the metallic sites on the catalyst surface, improving their efficiency in dehydrogenating the *n*-alkanes to *n*-alkenes (first step) and hydrogenating the *iso*-alkenes to the final *iso*-alkanes, therefore providing enhanced reaction rates and improved C_8 conversions. The increased reaction rates also affected the selectivity in favour of cracking products. The formation of such products (including *n*-propane, butane, and hexane) did not increase significantly on increasing the H_2 pressure up to 4–5 bar. A further increase in the H_2 pressure (>5 bar) led to a higher selectivity in favour of cracking products, especially C_2 to C_4 products. 3-Methylheptane was still preferentially produced in the reaction compared to 2- and 4-methylheptanes.

Table 5. Product distribution and selectivities in favour of cracking (S_{CK}, mol%), including selectivities for C_2 to C_4 (S_{C2-4}, mol%), pentane (S_{C5}, mol%), hexane (S_{C6}, mol%), and isomerisation to methylheptanes (S_{MH}, mol%), including 2-, 3-, and 4-methylheptanes (S_{XMH}, mol%), of supported platinum materials in the hydroisomerisation of *n*-octane.[a]

Catalyst	S_{CK}			S_{MH}			S_{OTHERS}	
	S_{C2-4}	S_{C5}	S_{C6}	S_{2MH}	S_{3MH}	S_{4MH}	S_{TOL}	S_{ETBZ}
0.5%Pt-40Al	10	5	3	22	37	15	6	1
0.5%Pt-30Al	18	8	2	19	33	13	3	–
0.5%Pt-20Al	7	7	3	22	39	14	5	3
0.5%Pt-15Al	15	8	3	20	35	15	4	–
0.5%Pt-SAPO11	22	10	1	28	18	13	7	1

[a] $T=375\,^{\circ}C$; $p=5$ bar, 0.1 g catalyst, $WHSV=12.7\ h^{-1}$; 4 h reaction.

The deactivation of the materials at atmospheric pressure (1 bar) was notable. This may be attributed to the formation of carbonaceous species on the catalyst surface, which contribute to the poisoning and/or blocking of the active centres

Table 6. Effect of the hydrogen pressure on the total conversion (X_T, mol %) and selectivities in favour of cracking (S_{CK}, mol %) and isomerisation to 3-methylheptane (S_{3MH}, mol %) and 2- and 4-methylheptanes (S_{2+4MH}, mol %) of 3 % Pt-40Al in the hydroisomerisation of *n*-octane.[a]

P_{H_2} [bar]	4 h reaction				12 h reaction				20 h reaction			
	X_T	S_{CK}	S_{3MH}	S_{2+4MH}	X_T	S_{CK}	S_{3MH}	S_{2+4MH}	X_T	S_{CK}	S_{3MH}	S_{2+4MH}
1	38	29	31	31	36	26	33	33	34	23	32	32
3	56	25	34	33	55	22	35	35	53	24	35	33
5	70	42	26	25	67	39	27	27	64	35	29	29
7	78	52	21	22	75	43	26	25	72	35	30	29

[a] $T = 375\,°C$, 0.1 g catalyst, $WHSV = 12.7\ h^{-1}$; the fact that the selectivities do not total 100 is due to toluene (traces of ethylbenzene were also obtained).

(Table 6). However, the stabilities of the supported Pt catalysts generally increase with increasing H_2 pressure in the reactor (Table 6).[8] In any case, the materials proved to be highly stable and the deactivation was almost negligible (< 10 % of the initial catalytic activity) after 20 h of reaction.

The temperature also had an important effect on the conversion and selectivity in these systems, increasing both the *n*-octane conversion and the selectivity in favour of cracking (Table 7), in good agreement with previously reported results.[8,9,18] These increases were only significant at H_2 pressures higher than 3 bar. 3-Methylheptane was obtained as the main reaction product, with a selectivity of around 30 % at temperatures below 400 °C. The platinum nanoparticles were found to be highly stable, even at high reaction temperatures (400 °C and over).

The Pt loading was another key parameter influencing the activity of the supported Pt materials (Table 8). An increase in the Pt loading (from 0.5 to 4 wt %) provided higher catalytic activities, but also led to the formation of increasing quantities of cracking products (mainly C_2 to C_4). This increase in selectivity in favour of short-chain alkanes was more significant at higher hydrogen pressures in the system (> 5 bar). Pt loadings over 4 wt % gave reduced activities, indicating a less well dispersed and heterogeneous particle distribution (with metal dispersions below 40 %) as well as a higher concentration of large Pt clusters in the materials (Figure 3C).

Conclusion

Highly active platinum nanoparticles dispersed on Al-MCM-48 have been prepared. The supported materials displayed a very narrow particle size distribution. The materials exhibited high activities and high selectivities in favour of C_7-branched isomers in the hydroisomerisation of *n*-octane. The production of 3-methylheptane was found to be favoured with respect to the 2- and 4-isomers, implying a shape-selectivity effect in the mesoporous supported Pt catalysts. The catalysts proved to be highly stable at high temperatures and high hydrogen pressures. They therefore offer a potentially interesting alternative to the traditional Pt, Pd, and Re/Al_2O_3 supported catalysts.

Acknowledgements

This research was subsidized by grants from the Dirección General de Investigación (Project CTQ2005-04080 and CTQ2007-65754/PPQ), the Ministerio de Educación y Ciencia, FEDER Funds, and the Consejería de Innovación, Ciencia y Empresa (Junta de Andalucia, Project FQM-191).

Table 7. Effect of the temperature on the total conversion (X_T, mol %) and selectivities in favour of cracking (S_{CK}, mol %) and isomerisation to 3-methylheptane (S_{3MH}, mol %) and 2- and 4-methylheptanes (S_{2+4MH}, mol %) of 3 % Pt-40Al in the hydroisomerisation of *n*-octane.[a]

T [°C]	4 h reaction				12 h reaction				20 h reaction			
	X_T	S_{CK}	S_{3MH}	S_{2+4MH}	X_T	S_{CK}	S_{3MH}	S_{2+4MH}	X_T	S_{CK}	S_{3MH}	S_{2+4MH}
350	28	22	34	35	27	17	38	37	23	15	39	42
375	70	42	26	25	67	39	27	26	64	35	29	28
400	82	60	15	16	78	57	16	20	75	52	17	25

[a] $p = 5$ bar; 0.1 g catalyst, $WHSV = 12.7\ h^{-1}$; the fact that the selectivities do not total 100 is due to toluene (traces of ethylbenzene were also obtained).

Table 8. Effect of the Pt loading of the material on the total conversion (X_T, mol %) and selectivities in favour of cracking (S_{CK}, mol %) and isomerisation to 3-methylheptane (S_{3MH}, mol %) and 2- and 4-methylheptanes (S_{2+4MH}, mol %) of Pt-40Al materials in the hydroisomerisation of *n*-octane.[a]

Pt (%)	4 h reaction				12 h reaction				20 h reaction			
	X_T	S_{CK}	S_{3MH}	S_{2+4MH}	X_T	S_{CK}	S_{3MH}	S_{2+4MH}	X_T	S_{CK}	S_{3MH}	S_{2+4MH}
0.5	50	18	37	38	48	17	39	39	48	18	39	38
1	54	32	31	30	50	32	31	30	49	20	38	37
3	70	42	26	25	67	39	27	26	64	35	32	30
5	61	37	29	26	57	35	28	29	55	36	29	27

[a] $T = 375\,°C$, $p = 5$ bar, 0.1 g catalyst; $WHSV = 12.7\ h^{-1}$; the fact that the selectivities do not total 100 is due to toluene (traces of ethylbenzene were also obtained).

[1] N. A. Cusher, P. Greenouch, J. P. K. Rolfe, J. A. Weiszmann, in *Handbook of Petroleum Refining Processes* (Ed.: R. A. Meyers), McGraw-Hill, New York, **1986**.
[2] V. M. Akhmedov, S. H. Al-Khowaiter, *Catal. Rev.* **2007**, *49*, 33–109.
[3] Z. B. Zhang, A. Kamo, T. Yonedo, T. Komatsu, T. Yashima, *Appl. Catal. A* **1997**, *159*, 119–132.
[4] E. Iglesia, D. G. Barton, S. L. Soled, S. Miseo, J. E. Baumgartner, W. E. Gates, G. A. Fuentes, G. D. Meitzner, *Stud. Surf. Sci. Catal.* **1996**, *101*, 533–540.
[5] S. I. Miller, US Patent 5135638, **1992**.
[6] Y. Liu, Y. Guan, C. Li, J. Lian, G. J. Gan, E. C. Lim, F. Kooli, *J. Catal.* **2006**, *244*, 17–23.
[7] P. Meriaudeau, V. A. Tuan, V. T. Nghiem, S. Y. Lai, L. N. Hung, C. Naccache, *J. Catal.* **1997**, *169*, 55–66.
[8] J. M. Campelo, F. Lafont, J. M. Marinas, *J. Chem. Soc. Faraday Trans.* **1995**, *91*, 1551–1555.
[9] J. M. Campelo, F. Lafont, J. M. Marinas, *J. Chem. Soc. Faraday Trans.* **1995**, *91*, 4171–4177.
[10] F. Alvarez, F. R. Ribeiro, G. Perot, C. Thomazeau, M. Guisnet, *J. Catal.* **1996**, *162*, 179–189.
[11] L. B. Galperin, *Appl. Catal. A* **2001**, *209*, 257–268.
[12] K. C. Park, S. K. Ihm, *Appl. Catal. A* **2000**, *203*, 201–209.
[13] F. C. Meunier, F. Cavallaro, T. Le Goaziou, A. Goguet, C. Rioche, *Catal. Today* **2006**, *112*, 64–67.
[14] D. G. Barton, S. L. Soled, G. D. Meitzner, G. A. Fuentes, E. Iglesia, *J. Catal.* **1999**, *181*, 57–72.
[15] E. Iglesia, S. L. Soled, G. M. Kramer, *J. Catal.* **1993**, *144*, 238–253.
[16] P. Perez-Romo, C. Potvin, J. M. Manoli, G. Djega-Mariadassou, *J. Catal.* **2002**, *205*, 191–198.
[17] J. Xu, J. Y. Ying, *Angew. Chem.* **2006**, *118*, 6852–6856; *Angew. Chem. Int. Ed.* **2006**, *45*, 6700–6704.
[18] I. Eswaramoorthi, V. Sundaramurthy, N. Lingappan, *Microporous Mesoporous Mater.* **2004**, *71*, 109–115.
[19] K. Chaudhari, T. K. Das, A. J. Chandwadkar, S. Sivasanker, *J. Catal.* **1999**, *186*, 81–90.
[20] A. Hollo, J. Hancsok, D. Kallo, *Appl. Catal. A* **2002**, *229*, 93–102.
[21] S. Gopal, P. G. Smirniotis, *Appl. Catal. A* **2003**, *247*, 113–123.
[22] R. Roldan, F. J. Romero, C. Jiménez-Sanchidrian, J. M. Marinas, J. P. Gomez, *Appl. Catal. A* **2005**, *288*, 104–115.
[23] P. N. Kuznetsov, *J. Catal.* **2003**, *218*, 12–23.
[24] Z. Wang, Z. Tian, F. Teng, G. Wen, Y. Xu, Z. Xu, L. Lin, *Catal. Lett.* **2005**, *103*, 109–116.
[25] J. M. Campelo, D. Luna, R. Luque, J. M. Marinas, A. A. Romero, J. J. Calvino, M. P. Rodríguez-Luque, *J. Catal.* **2005**, *230*, 327–338.
[26] V. L. Budarin, J. H. Clark, R. Luque, K. Milkowski, D. J. Macquarrie, R. J. White, PCT Patent, WO 2007104798 A2 20070920, 2007.
[27] J. C. Vartuli, K. D. Schmitt, C. T. Kresge, W. J. Roth, M. E. Leonowicz, S. B. McCullen, S. D. Hellring, J. S. Beck, J. L. Schlenker, D. H. Olson, E. W. Sheppard, *Chem. Mater.* **1994**, *6*, 2317–2326.
[28] M. Lashdaf, V. V. Nieminen, M. Tiita, T. Venäläinen, H. Österholm, O. Krause, *Microporous Mesoporous Mater.* **2004**, *75*, 149–158.
[29] P. Gallezot, G. Bergeret, *Handbook of Heterogeneous Catalysis, Vol. 2* (Eds.: G. Ertl, H. Knözinger, J. Weitkamp), Wiley-VCH, Weinheim, **1997**, 441.
[30] G. Xiong, N. Yao, W. Han, S. Sheng, W. Yang, *Cuihua Xuebao* **2005**, *26*, 759–762.
[31] F. M. Bautista, J. M. Campelo, A. Garcia, D. Luna, J. M. Marinas, A. A. Romero, J. A. Navio, M. Macias, *J. Catal.* **1994**, *145*, 107–125.
[32] R. Beecher, A. Voorhies, P. Eberly, *Ind. Eng. Chem. Prod. Res. Dev.* **1968**, *7*, 203–209.
[33] A. Chica, A. Corma, *J. Catal.* **1999**, *187*, 167–176.
[34] J. F. Kriz, T. D. Pope, M. Stanciulescu, J. Monnier, *Ind. Eng. Chem. Res.* **1998**, *37*, 4560–4569.
[35] P. Sanchez, F. Dorado, M. J. Ramos, R. Romero, V. Jiménez, J. L. Valverde, *Appl. Catal. A* **2006**, *314*, 248–255.
[36] F. E. Condon, Stepwise reaction on separate catalytic centers. Catalysis, *Vol. 6* (Ed.: P. H. Emmet), Reinhold, New York, pp. 121.
[37] D. M. Brouwer, H. Hogeveen, *Prog. Phys. Org. Chem.* **1972**, *9*, 179–184.
[38] J. Weitkamp, *Ind. Eng. Chem. Prod. Res. Dev.* **1982**, *21*, 550–558.
[39] A. de Lucas, J. L. Valverde, P. Sanchez, F. Dorado, M. J. Ramos, *Appl. Catal. A* **2005**, *282*, 15–24.

Received: January 29, 2008
Published online: May 15, 2008

